IN-02
62504
p- 11

NASA Technical Memorandum 107023

Investigation of Water Droplet Trajectories Within the NASA Icing Research Tunnel

Andrew L. Reehorst
Lewis Research Center
Cleveland, Ohio

and

Mounir Ibrahim
Cleveland State Unviversity
Cleveland, Ohio

Prepared for the
International Icing Symposium '95
cosponsored by the American Helicopter Society
and Society of Automotive Engineers
Montreal, Canada, September 18–21, 1995

National Aeronautics and
Space Administration

(NASA-TM-107023) INVESTIGATION OF WATER DROPLET TRAJECTORIES WITHIN THE NASA ICING RESEARCH TUNNEL (NASA. Lewis Research Center) 11 p

N95-32769

Unclas

G3/02 0062504

Investigation of Water Droplet Trajectories Within the NASA Icing Research Tunnel

Andrew L. Reehorst
NASA Lewis Research Center
Cleveland, Ohio 44135

and

Mounir Ibrahim
Cleveland State University
Cleveland, Ohio 44115

Abstract

Water droplet trajectories within the NASA Lewis Research Center's Icing Research Tunnel (IRT) were studied through computer analysis. Of interest was the influence of the wind tunnel contraction and wind tunnel model blockage on the water droplet trajectories. The computer analysis was carried out with a program package consisting of a three-dimensional potential panel code and a three-dimensional droplet trajectory code. The wind tunnel contraction was found to influence the droplet size distribution and liquid water content distribution across the test section from that at the inlet. The wind tunnel walls were found to have negligible influence upon the impingement of water droplets upon a wing model.

Nomenclature

2-D	Two-Dimensional
3-D	Three-Dimensional
Beta	Local water collection efficiency, dimensionless
IRT	Icing Research Tunnel
LWC	Liquid Water Content, g/m^3
MVD	Mean Volumetric Diameter, microns

Introduction

The growth of ice on aircraft has been a problem since the time that aircraft first began flying by instruments into visible moisture. Over the years several methods have been developed to examine and hopefully control the aircraft ice accretion process. Data was first obtained by personal accounts of pilots that were unfortunate enough to stray into the icing environment. Later, flight test personnel purposely attempted to accrete ice on their aircraft by flying into known icing conditions. Flight testing is both hazardous, time-consuming, and expensive. To provide controlled testing conditions, refrigerated wind tunnels with water spray systems were developed. This new capability provided a new means to gain better understanding of the icing phenomenon and develop improved ice protection systems. But even wind tunnel testing can be quite expensive and is not fully compatible with all initial design efforts. Computer analysis provides a powerful tool for engineers during the early phases of design. Initially, mechanical machines were used to predict the flow field and water

droplet trajectories around various aerodynamic surfaces. With the advancement of digital computers, the mechanical machines were quickly displaced. By the mid-1980's several computer codes were developed to calculate the flow field and water droplet trajectories about arbitrarily shaped bodies. The first codes were strictly 2-D in nature. Today, several codes are capable of performing these calculations for arbitrary 3-D surfaces. Due to these advancements one may now use these computational tools to study the icing wind tunnels. What are the effects of the wind tunnel's contraction upon the water droplet trajectories and the distribution of water droplets in the test section? How can one compare the water impingement from the wind tunnel's artificial icing cloud contained within the tunnel walls to that of a natural icing cloud impinging upon a wing with no surrounding walls? These are the questions that may be now answered with the help of computer analysis and will be addressed in this paper. A more detailed description of this effort is also available[1], this includes derivations of important aspects of the computer codes, comparisons to experimental data and accuracy studies.

Several individuals have examined the problems associated with introducing an artificial cloud within a wind tunnel. Wells and Bragg[2] performed a 2-D computational study to examine the effect of straight wind tunnel walls on droplet trajectories impinging upon an airfoil model. This study compared flow field and droplet trajectory calculations for an airfoil with wind tunnel walls to no-wall calculations and showed that the far-field upwash and near-field downwash effects canceled and resulted in similar water droplet collections on the airfoil. Khodadoust and Bragg[3] examined the 2-D effect of a wind tunnel contraction on an artificial icing cloud. They found that the aerodynamics introduced by the contraction acted as a droplet size sorting device (moving larger droplets towards the center of the wind tunnel) and tended to contract the overall cloud significantly.

The 3-D code selected for the flow field calculations was VSAERO[4,5,6]. It is a low-order panel method that includes wake and boundary layer modeling. This code was modified and extended from its original use as an external flow solver to more general use that includes internal flows. The use of VSAERO for internal flows is described for several applications by Ashby and Sandlin[7], Nathman and Frank[8], and Carlin and Bevan[9].

The computer code ICE was selected for the calculation of the water droplet trajectories for this effort[10] because it is closely coupled with VSAERO. ICE relies on both the VSAERO aerodynamic solution and geometry definition in the form of the VSAERO plot file.

Examination of tunnel contraction influence on trajectories

Computer Code Inputs

VSAERO was run with the uniform inlet velocity set to provide a test section non-dimensional velocity of 1.0. With this flow field solution available, ICE was run to predict the water droplet trajectories for droplet sizes ranging from 5.539 microns to 65.084 microns and test section velocity of 67 m/s (150 mph). The droplet size distribution used was the seven bin distribution for a 20.0 micron

spray from a NASA standard icing nozzle. The droplets were released in a square grid pattern with a 0.3 m (1 ft) spacing.

Results

To examine the influence of the wind tunnel contraction upon the water droplet trajectories, the analysis methodology developed by Khodadoust and Bragg[3] was employed. The water concentration in the test section was calculated for each droplet size by dividing the upstream area defined by four adjoining trajectories (0.09 m^2 (1 ft^2)) by the similar area at the test section center. To obtain an idea of the water mass distribution, this value was then divided by the tunnel's area contraction, 14.13255. The resultant concentration (or relative LWC) for several droplet size across the test section are shown in Figures 1, 2, and 3 (these and following plots represent a quarter of the test section with the origin of the coordinate system located at the tunnel centerline). At this point the water concentrations have not been weighted by the droplet size distribution. For comparison, the relative LWC for droplets not influenced by the wind tunnel walls would be 1.0. With that in mind, one can see that as the droplet size increases the droplets are forced closer towards the center of the tunnel, increasing the relative LWC there. To maintain a mass balance, this also indicates that the outer boundary of the droplet cloud contracts with increasing droplet size.

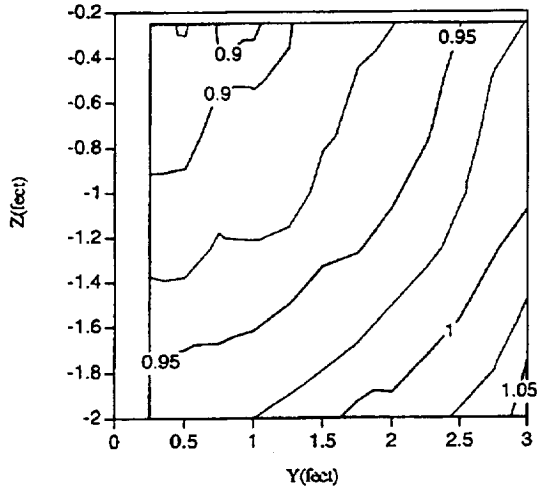

Figure 1 Computed relative LWC's for droplet size of 5.5 microns

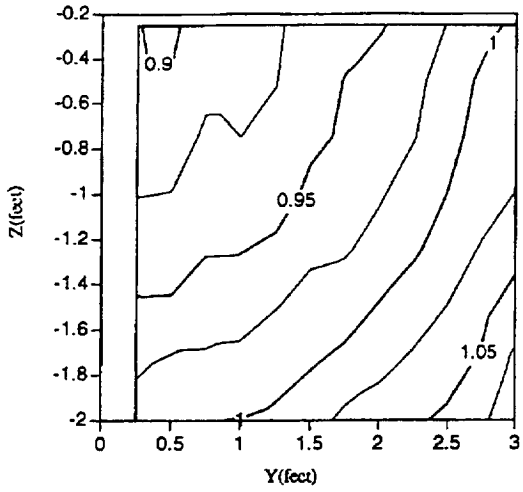

Figure 2 Computed relative LWC's for droplet size of 20 microns

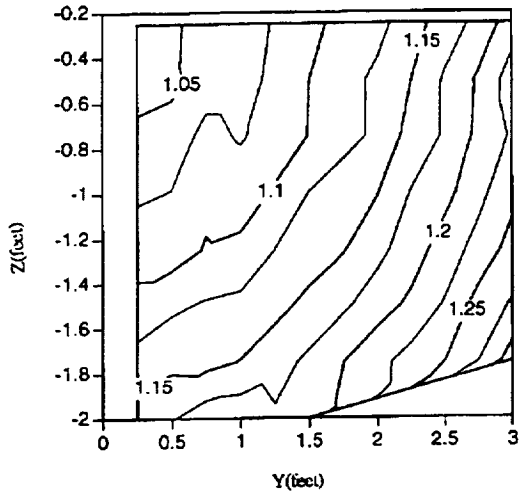

Figure 3 Computed relative LWC's for droplet size of 65.1 microns

Due to the influence of the tunnel contraction, the distribution of water as a function of droplet size varies across the test section. This is shown in Figure 4 which plots the water concentration distribution at the point closest to the wind tunnel center, the center of the region of interest, and the point furthest from the wind tunnel center. For comparison, the NASA standard nozzle distribution is also plotted. The area under these distributions represents the total amount of water present at the respective test section location. A plot of the total water distribution (effective LWC) is shown in Figure 5. Within the area of interest examined here, the effective LWC is seen to vary by approximately +/-7.5 percent.

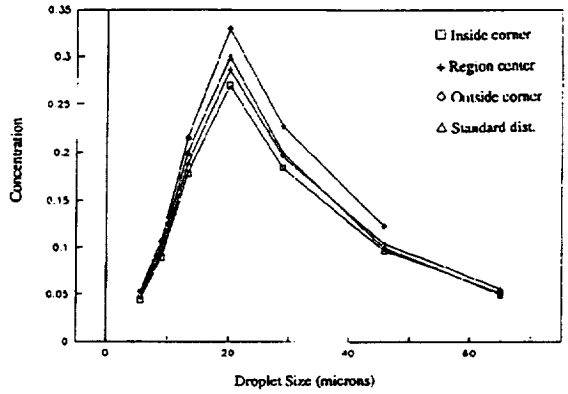

Figure 4 Water concentration versus droplet size

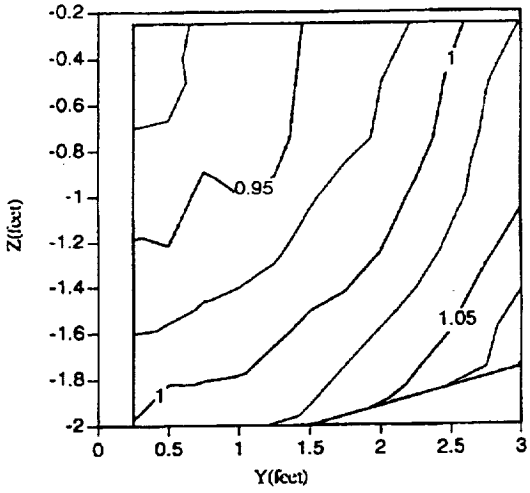

Figure 5 Effective LWC

To examine the variation of MVD across the test section, it is first required that the water concentration distribution seen in Figure 4 be non-dimensionalized by the effective LWC for each point in space. This results in the water concentration distributions seen in Figure 6. These distributions are for the same locations examined in Figure 4. For the entire region of interest, the calculated water concentration distributions are seen to vary from that of the NASA standard nozzle, which indicates that the MVD will in fact be influenced.

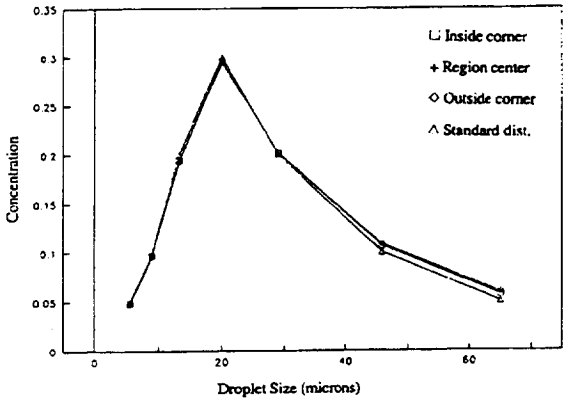

Figure 6 Non-dimensionalized water concentration versus droplet size

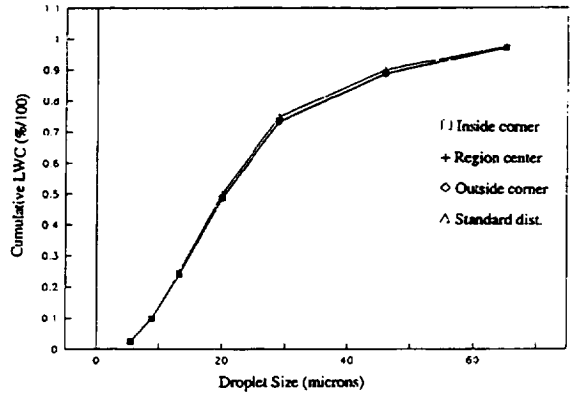

Figure 7 Cumulative LWC versus water droplet size

To calculate the MVD at a given location, the cumulative LWC as a function of droplet size must first be determined. This is shown in Figure 7. The MVD is then determined by finding the droplet size at the 50 percent point of the cumulative LWC curve. The plot of the resultant effective MVD distribution is shown in Figure 8. Since the spray bar plane droplet distribution represented a 20.0 micron MVD, the test section MVD was raised by 0.35 microns near the tunnel center and by 0.45 near the outer edge of the area examined. This increase in MVD is due to the increase in the number of large droplets in this region as seen earlier. A related decrease in MVD would be expected near the test section walls due to the decrease in the number of large droplets in that region.

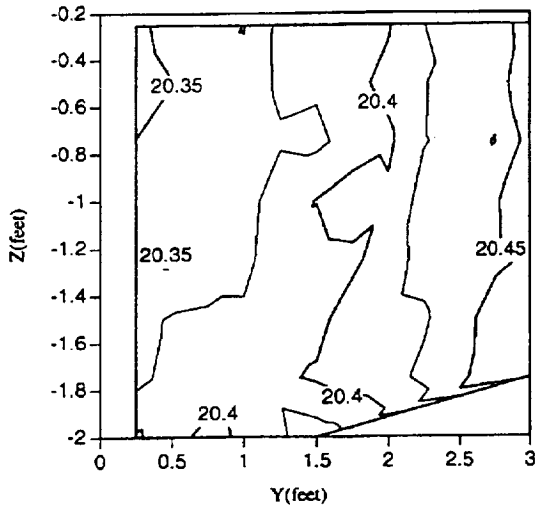

Figure 8 Effective MVD

This series of calculations was also carried out for a test section velocity of 134 m/s (300 mph). As would be expected, the droplet cloud continues to contract as the wind tunnel velocity is increased. Within the area of interest, the effective LWC for this tunnel condition is seen to vary from about -7 to +10 percent. And the MVD is elevated by between 0.45 and 0.7 microns from the initial value of 20.0 microns.

Examination of tunnel wall influence on trajectories

Similar inlet conditions were utilized for the calculations that included a model in the test section. The model paneled was a section of DeHavilland Twin Otter wing spanning the wind tunnel test section from floor to ceiling. The actual wind tunnel model was constructed from a piece of aircraft wing, so it is quite large with respect to the IRT's test section area, 2.0 m (78 in) chord with a 16 percent thickness. Specific care must be exercised when including a model in the wind tunnel paneling to ensure panel matching and ensure no "leaks" develop that would influence the aerodynamic solution.

Figures 9 and 10 show the calculated pressure distributions about the Twin Otter wing installed in the IRT test section for 0 and 4 degrees angle-of-attack respectively. Figures 11 and 12 show similar results for the Twin Otter wing with no wind tunnel walls and a span of 12.2 m (40 ft). By comparing the plots it becomes obvious that the pressure distribution about the Twin Otter wing is significantly influenced by the presence of the wind tunnel wall. As would be expected, this influence increases as the model's angle-of-attack is increased. A simple 2-D wall correction calculation was completed using a technique described by Rae and Pope[11] to correct the lift calculated for the installed wing. When compared to the calculated lift for the isolated wing the error was only 3.3%.

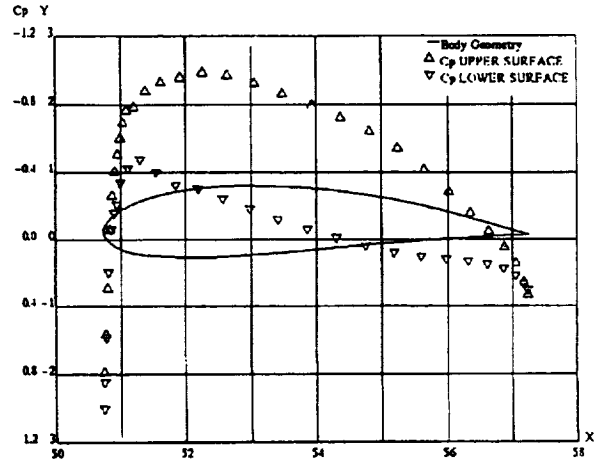

Figure 9 Pressure distribution on installed Twin Otter wing at 0 degrees angle-of-attack

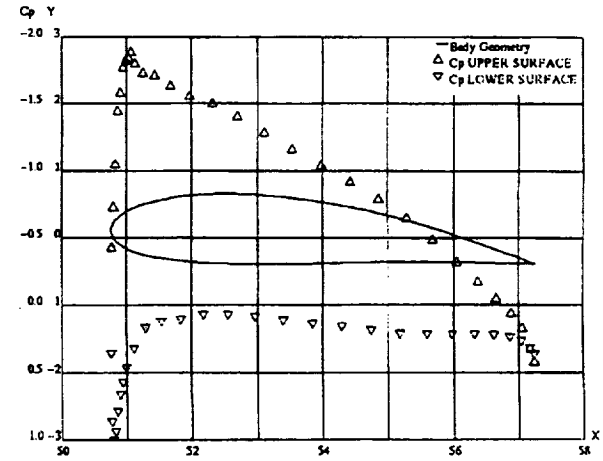

Figure 10 Pressure distribution on installed Twin Otter wing at 4 degrees angle-of-attack

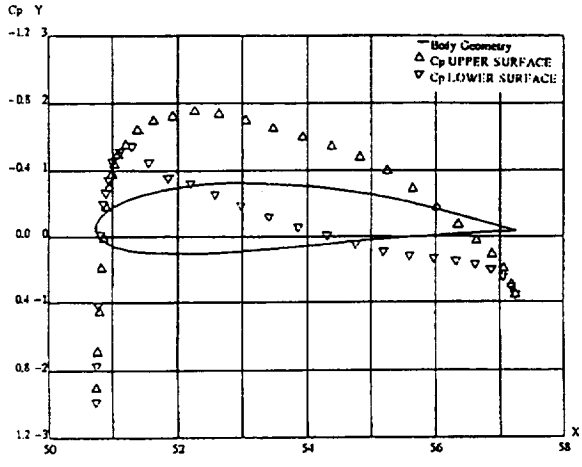

Figure 11 Pressure distribution on isolated Twin Otter wing at 0 degrees angle-of-attack

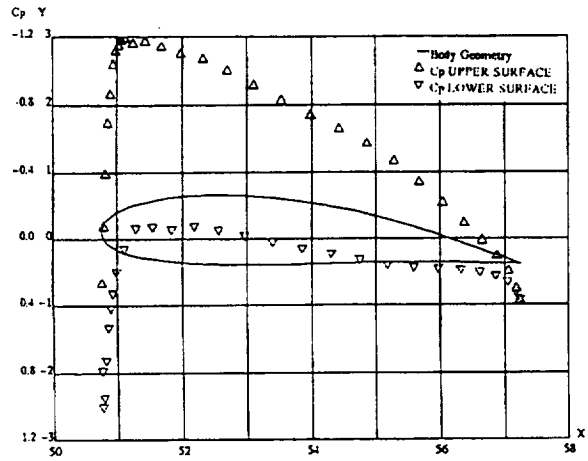

Figure 12 Pressure distribution on isolated Twin Otter wing at 4 degrees angle-of-attack

The water droplet collection efficiency (beta) was calculated with ICE for these geometries. The first cases to be examined were the installed and isolated wing at four degrees angle-of-attack. Figure 13 shows the results for a 20 micron MVD droplet distribution when the droplets were released at station X=2.3 m (7.7 ft) (which represents the spray bar plane in the IRT). Because the installed droplets are originating in the settling chamber, the betas for this case were corrected by the wind tunnel contraction ratio, 14.13. Overall, the two curves agree well, with the maximum beta and the impingement limits agreeing very well and only a slight dip for the installed wing just below the maximum beta point.

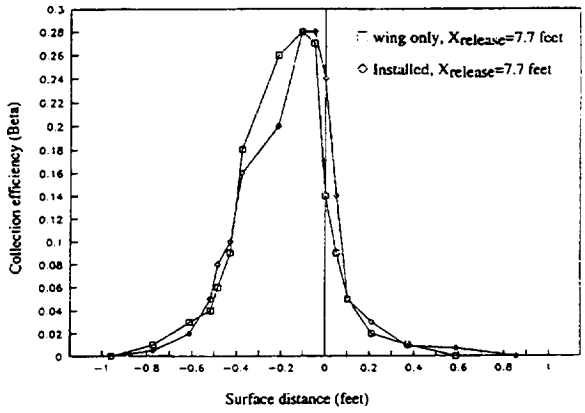

Figure 13 Water droplet collection efficiency on the Twin Otter wing both installed in the IRT and isolated, at 4 degrees angle-of-attack for 20 micron MVD droplet distribution

The agreement demonstrated between the installed and isolated wing cases is very interesting considering the difference seen in the pressure distributions for the two geometries. Even more interesting is the level of agreement when the trajectories themselves are observed. Figure 14 shows the impingement limit trajectories for the two geometries at 4 degrees angle-of-attack with a 20 micron droplet cloud. The effect of the wind tunnel contraction upon the installed wing's trajectories is very evident in the region up to roughly X=12.2 m (40 ft). The differences beyond this point are due to straight-wall effects. Both the beta curve agreement and the trajectory merging were also observed by Wells and Bragg[2]. They concluded that the far-field

and near-field upwash effects canceled. The near-field (less than 1/10 chordlength ahead of the model) upwash increases as the wind tunnel walls are brought closer to the model and the far-field (greater than one chordlength ahead of the model) upwash decreases as the walls are brought closer. The Wells and Bragg results were for long parallel walls, so it is very significant that the trends hold true for this IRT data since the IRT contraction ends just one chordlength ahead of the Twin Otter wing model.

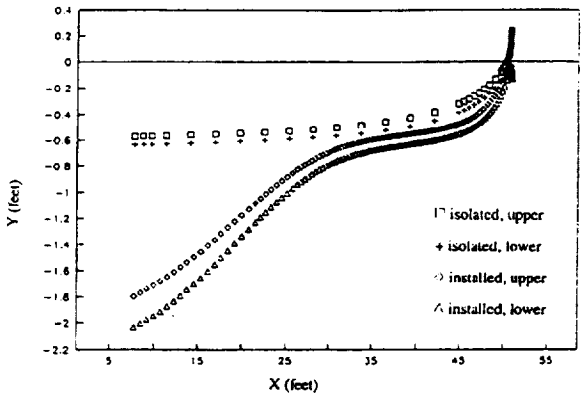

Figure 14 Impingement trajectories for installed and isolated Twin Otter wing at 4 degrees angle-of-attack for 20 micron droplets

Figure 15 shows the water droplet collection efficiency curves calculated for the isolated and installed wing at zero degrees angle-of-attack with a 20 micron MVD droplet cloud distribution. The lower impingement limits for the two curves match and the upper limits are within one panel width. The shape of the two curves are close except for the higher maximum beta for the installed wing case. The spike in this plot is likely due to inadequate panel resolution at this point which influenced calculation of the off-body velocity. The difference in the curves near the upper impingement limit is again likely tied to panel resolution. Error is introduced to the particle trajectory as it passes near panel edges. Due to the Twin Otter wing geometry, at zero degrees angle-of-attack, droplets are skimming the wing's forward-facing upper surface. This means that the droplet trajectories are passing very close to several panel edges. The error in the calculated trajectories is also increased since the panels in this region are larger than those near the stagnation point. Also, due to wall effects the velocities in this region are greater for the installed wing than for the isolated wing, and this will amplify any velocity error. While the errors that arose in these calculation do not make it the best validation candidate, the results for the zero degree cases do support the findings from the four degree cases.

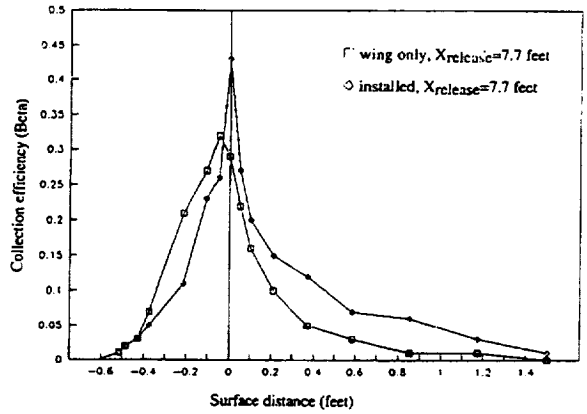

Figure 15 Water droplet collection efficiency on the Twin Otter wing both installed in the IRT and isolated at 0 degrees angle-of-attack for 20 micron MVD droplet distribution

Conclusions

The methodology developed by Khodadoust and Bragg[3] for 2-D analysis of the effects of a wind tunnel contraction upon droplet